Journal of Applied Polymer Science

Effects of size and shape originated synergism of carbon nano fillers on the electrical and mechanical properties of conductive polymer composites

Alper Kasgoz,[1,2] Dincer Akın,[1] Ali Durmus[1]

[1]Faculty of Engineering, Istanbul University, Department of Chemical Engineering, 34320, Avcılar Istanbul, Turkey

[2]Faculty of Engineering, Yalova University, Faculty of Engineering, Polymer Engineering Department, 77100, Yalova, Turkey

Correspondence to: A. Durmus (E-mail: durmus@istanbul.edu.tr)

ABSTRACT: In this study, microstructural features, mechanical properties, and electrical conductivity behaviors of thermoplastic composites prepared by using of cyclic olefin copolymer (COC) as matrix and various types of carbon nano materials, expanded graphite (EG), carbon nanofiber (CNF), and multi walled carbon nanotubes (CNT) as conductive fillers were investigated. Effects of using of double and triple filler combinations on the electrical properties of composites were also quantified in detail by measuring the bulk resistance of samples under alternating current with an impedance spectrometer. The electrical percolation values of fillers were found to be 20, 10, and 5 phr for the series of composites prepared with the EG, CNF, and CNT, respectively. It was obtained that the bulk resistances of percolated samples were dramatically decreased from 10^{14} ohm.cm to $10^{3}-10^{4}$ ohm.cm. On the other hand, it was also found that the using of double and triple filler combinations provided much lower (about 10^{1} ohm.cm) bulk resistance which corresponded to higher conductivity values than the highly filled composites including of 30 and 40 phr of EG. Based on the DMA measurements and the quantifying of elastic modulus values of composites in the rubbery region, it was found that the reinforcing effects of carbon nano fillers on the elastic modulus of composites decreased in the order of CNT>CNF>EG, depending on the aspect ratio (A_f) values of fillers into the matrix. © 2015 Wiley Periodicals, Inc. J. Appl. Polym. Sci. **2015**, *132*, 42313.

KEYWORDS: composites; extrusion; mechanical properties; structure-property relations

Received 15 January 2015; accepted 5 April 2015

DOI: 10.1002/app.42313

INTRODUCTION

Thermoplastic-based conductive polymer composites (CPCs) have recently attracted great interest in many applications such as batteries, bipolar plates, sensors, and actuators, electromagnetic interference (EMI) shielding materials, due to good processability, tunable mechanical and thermal properties, low cost, and wide range of applications.[1–4] It is a well-known fact that the commonly used and commercially available thermoplastic polymers and thermoset resins are normally insulating materials which possess extremely high resistivity. Some electrically conductive polymers such as polyacetylene, polypyroles, polythiophenes, polyaniline, poly(pheneylene sulfide) etc. have been considered as new generation polymers which can be possibly used in conductive applications. Although conductive polymers consist of structural units that available electron transfer throughout the chain or bulk structure, difficulties in mass production, processability, adaptation to industrial processes, and high cost can be regarded as some technical drawbacks of these polymers for conductive material applications. Introducing of various types of electrically conductive fillers like metal[5–7] and carbon powders[8–10] into thermoplastics is easy and versatile method to prepare CPCs. Particularly, carbon nano fillers are widely preferred materials for producing of CPCs because they can provide higher electrical conductivity and improve the mechanical properties of CPCs by using of relatively lower amount of filler compared to other types of carbon materials.

Preparation of CPCs by using several types of carbon nano fillers such as carbon black (CB), single or multi-walled carbon nanotube (CNT), graphene (G), and graphene derivatives and investigation of their electrical and physical properties have been extensively studied.[11–22] Based on the physical property and electrical conductivity data reported in these works, CNT and graphene can be especially classified as high performance fillers since they allow preparing of CPCs with enhanced properties. However, lack of mass production and high-cost of CNT and graphene preclude extending of industrial using of these fillers in low-cost composite formulations and commercial applications. Hence, different formulation and processing

Table I. Some Physical Properties of the Materials Used in the Study

	Commercial names of the materials			
	COC	EG	CNF	CNT
Property	TOPAS® 5013	TIMREX® BNB 90	Pyrograf®-III PR-24 LHT	Aldrich 724769
Density (g/cm^3)	1.02	2.24	1.95	2.10
T_g (°C)[a]	135			
MVR (ml/10 min.)[b]	48			
Particle size (μm)[c]		85	*d*:100 nm *L*: >100 μm	d_{tube}: 6–9 nm *L*: 5 μm
Surface area (m^2/g)[c]		28.4	35–45	
OAN (ml/100 g)[d]		150		

[a] Glass transition temperature measured with DSC.
[b] Volumetric melt flow rate (ISO 1133).
[c] Average values declared by the producers.
[d] Oil absorption number (ASTM D2414).

approaches have been developed to prepare cost-effective CPCs including nano fillers. One of these methods is to use immiscible polymer blends as composite matrix instead of single phase polymer. It has been reported that higher conductivity values and lower percolation threshold could be obtained by this method compared to single phase matrix composites.[10,23,24] In the immiscible blend method, formation of selective localization of conductive filler into one of the components provides intense domains and a definite continuum phase in the bulk structure which yields higher conductivity by using of less amount of filler.[25] The most prominent disadvantage of the method is possibly deteriorating of other thermal and/or physical properties of CPCs by using a relatively high amount of secondary polymeric component due to the difference in physical properties of components and immiscibility issue between phases.

Another widely used method for the preparation of low-cost CPCs is using of multiple combinations of conductive fillers into a polymer matrix.[26–29] In this method, relatively low-cost and commercially available macro and nano fillers are generally used together into CPC formulations for attaining higher conductivity values than the single filler counterparts at a particular loading amount of filler. This phenomenon is called as "synergic effect of filler" and based on the augmenting of filler contacts to form higher number of conducting pathway. Clingerman *et al.*[30] prepared polycarbonate and nylon 6,6 based composites containing two and three kinds of carbon fillers such as CB and carbon fibers (CF) and synthetic graphite (SG) and showed that the combination of fillers resulted in a positive synergism on conductivity of polymer composite. On the other hand, investigation of electrical properties of CPCs depending on the variation of compositional and microstructural properties, specifically aspect ratio, dispersion and orientation of fillers, polymer-filler, and filler-filler interactions etc., of these materials is another important research area.[31–34]

In this study, thermoplastic-based CPCs including single, double, and triple combinations of various types of nano size and commercially available carbon fillers namely expanded graphite (EG), carbon nanofiber (CNF), and multi walled CNT were prepared with melt processing method. Electrical and mechanical properties of samples were quantified depending on the composite composition. Main goal of the study was to prepare low-cost CPCs having low resistance by using filler combinations and industrial processing methods. Thermoplastic matrix employed in the study was cyclic olefin copolymer (COC), a member of new types of high performance and amorphous engineering thermoplastics obtained via copolymerization of ethylene and norbornene. To the best of our knowledge, only a few studies have been previously reported on the preparation and characterization of COC composites filled with carbon based fillers.[15,35–38]

EXPERIMENTAL

Materials

The COC used in this study was a commercial grade copolymer, Topas® 5013, kindly donated by TOPAS. Carbon nano fillers employed in the composite formulations were EG (TIMREX® BNB90) kindly provided by TIMCAL (Switzerland), CNF purchased from Pyrograf®-III (PR-24-XT-LHT), and CNT supplied from Sigma-Aldrich (Product Code: 724769). Some physical properties of the polymer and fillers are listed in Table I.

Sample Preparation

Composites were prepared by the melt processing method in a lab-scale, co-rotating twin screw extruder (Rondol Micro Lab., UK, D: 10 mm, L/D: 20) with a screw speed of 70 rpm. Intermeshing screws of the extruder were configured as including 3D of 4×60° followed by 2D of 4×90° kneading segments. A temperature profile of 190–220–230–230°C was applied throughout the barrel from the feeding zone to die. A rod die with the diameter of 2 mm was used and the extrudates were granulated. Before the melt processing, all materials were dried in a vacuum oven overnight at 70°C. The materials were first dry mixed then loaded into the extruder barrel. For conductivity and dynamic mechanical tests, specimens (50 × 10 × 1 mm in length, width, and thickness) were prepared by compression molding under the pressure

of 7 MPa at 220°C. The composite granules were first heated up to molding temperature in the mold cavity without a pressure for about 10 min to melt the sample granules then the compression pressure was applied to sample for 5 min. The mold was then quickly transferred to a cold pressure equipped with a water-chiller and the same molding pressure was applied to the mold in the second pres for 5 min. The average cooling rate was about 40°C/min. The volume fraction of filler (ϕ_f) was calculated according to the following formula;

$$\varphi_f = \frac{\rho_p \times w_f}{\rho_f \times w_p + \rho_p \times w_f} \quad (1)$$

where ρ_p and ρ_f are the density values and w_p and w_f are the weight fractions of polymer and filler, respectively. Sample notation specifies kind and amount of fillers. Accordingly, abbreviation at the notation represents the filler type (e.g. EG, CNF, and CNT) and the given number refers the amount of filler as phr, part of filler per hundred of polymer. For example, CNF10 denotes the composite containing 10 phr of CNF or EG20CNF10 defines the sample composition including 20 phr of EG and 10 phr of CNF.

In this study, no compatibilizer or modifying agent were used in the composite structure because the main goal of the work is to investigate the effect of geometrical features and the amount of fillers on the electrical conductivity of samples. It is a well-known fact that a compatibilizer as a third component in the formulation or modification of filler surfaces via chemical or physical methods enhances the mechanical properties of CPCs by increasing of interfacial interactions between polymer and filler phases but, such materials affect the conductivity performances of CPCs negatively.

Scanning Electron Microscopy (SEM) Study

Micro-structural features of fillers and composites were investigated by a field emission scanning electron microscope (FE-SEM, FEI Quanta FEG 450) operated at 30 kV. Fillers in powder form were directly imaged and cryo-fractured surfaces of composite specimens into liquid nitrogen were imaged in the electron microscope after a proper sample preparation, sputter coating with metal.

Electrical Conductivity Measurements

Electrical conductivity measurements were carried out an impedance spectroscopy analyzer (Solartron SI 1260 Impedance/gain-phase analyzer and Solartron dielectric interface 1296 devices) which works with alternative current (AC) at 100 mV within the frequency range of 10^0-10^6 Hz. Test specimens for the conductivity measurements, a rectangular bar (20×10 mm) with the thickness of 2 mm, were prepared by compression molding in a hot press at 220°C. The same molding procedure explained before was applied to the composite granules to prepare the test specimens for the impedance measurements. Then, the test specimens were directly contacted with electrodes by coating with a conductive silver paste to provide better surface contact. All measurements were carried out at the room temperature and moisture.

Dynamic Mechanical Analysis (DMA)

Solid state viscoelastic properties of the samples were tested in a dynamic mechanical analyzer (DMA, ExStar 6100, SII Nanotechnology, Japan). The DMA tests were performed in tension mode at a frequency of 1.0 Hz and the temperature range of 20–200°C with the heating rate of 2°C min^{-1}.

RESULTS AND DISCUSSION

Microstructural Features of Fillers and Composites

SEM images of the fillers are given in Figure 1. Figure 1(a,b) show the layered and transparent structure of graphene sheets which implies that EG consisting of large and nano-thick graphene stacks. Figure 1(c,d) represent the microstructure of CNF. As seen in the Figure 1(c), the bundle form of CNF is a large particle. Average size of a cocoon-like bundle of CNF was determined as 35–60 μm. Figure 1(d) demonstrates the transparency of CNF structure at a higher magnification. Figure 1(e,f) show the SEM images of the CNT taken at different magnifications. It is seen that the CNT formed spherical bundles having the average size of 15 μm which were smaller than that of CNF particle.

The SEM micrographs of EG10, CNF10, and CNT5 samples were given in Figure 2. It can be clearly seen in the Figures 2(c–f) that the bundles of one dimensional (1D) fillers, CNF, and CNT, were substantially disentangled and dispersed into the polymer phase possibly due to the effects of intensive shear forces during melt processing. It is easy to distinguish single nanotubes and nanofibers embedded into the polymer matrix in the given images. Average diameter of CNF and CNT was determined as 125±18 nm and 43±3 nm, respectively. But, the lengths of these fillers cannot be measured on the examined cross-sections of samples since the large part of the nanofibers and nanotubes are embedded into the polymer matrix. Therefore, it is difficult to determine the aspect ratio (A_f) values, an indicative parameter for the dispersion quality of fillers in composite systems defined as the ratio of length (l) of a filler particle to its thickness (h) or diameter (d), of one dimensional fillers based on the SEM analysis, directly. On the other hand, the A_f values of CNF and CNT can be theoretically calculated by using the fiber and tube diameters observed in the SEM images and the lengths of the fillers declared by the producers by neglecting agglomeration issues. The theoretical A_f values of CNF and CNT were determined as 800 and 115, respectively by taken the fiber length as 100 μm and tube length as 5 μm. It can be deemed that the theoretical A_f value of CNF is quite high. This approach could also bring about inaccuracy because the extrusion process would break down the fibers and tubes. Therefore, the A_f values of CNF and CNT will be determined, and discussed in the next part, by testing the mechanical properties of composites. Morphological features of EG10 sample are shown in Figure 2(a,b). In these images, it is seen that the nano-thick EG sheets are dispersed in the polymer matrix homogenously.

Figure 3 shows the microstructural features of samples including double and triple filler combinations. Figure 3(a,b) illustrate the SEM micrographs of the EG20CNF10 and EG20CNT10, respectively. These figures indicate that the filler dispersion is still individually homogenous in the composites prepared with double filler like the samples containing single filler. Another important observation is that the using of 1D and 2D fillers

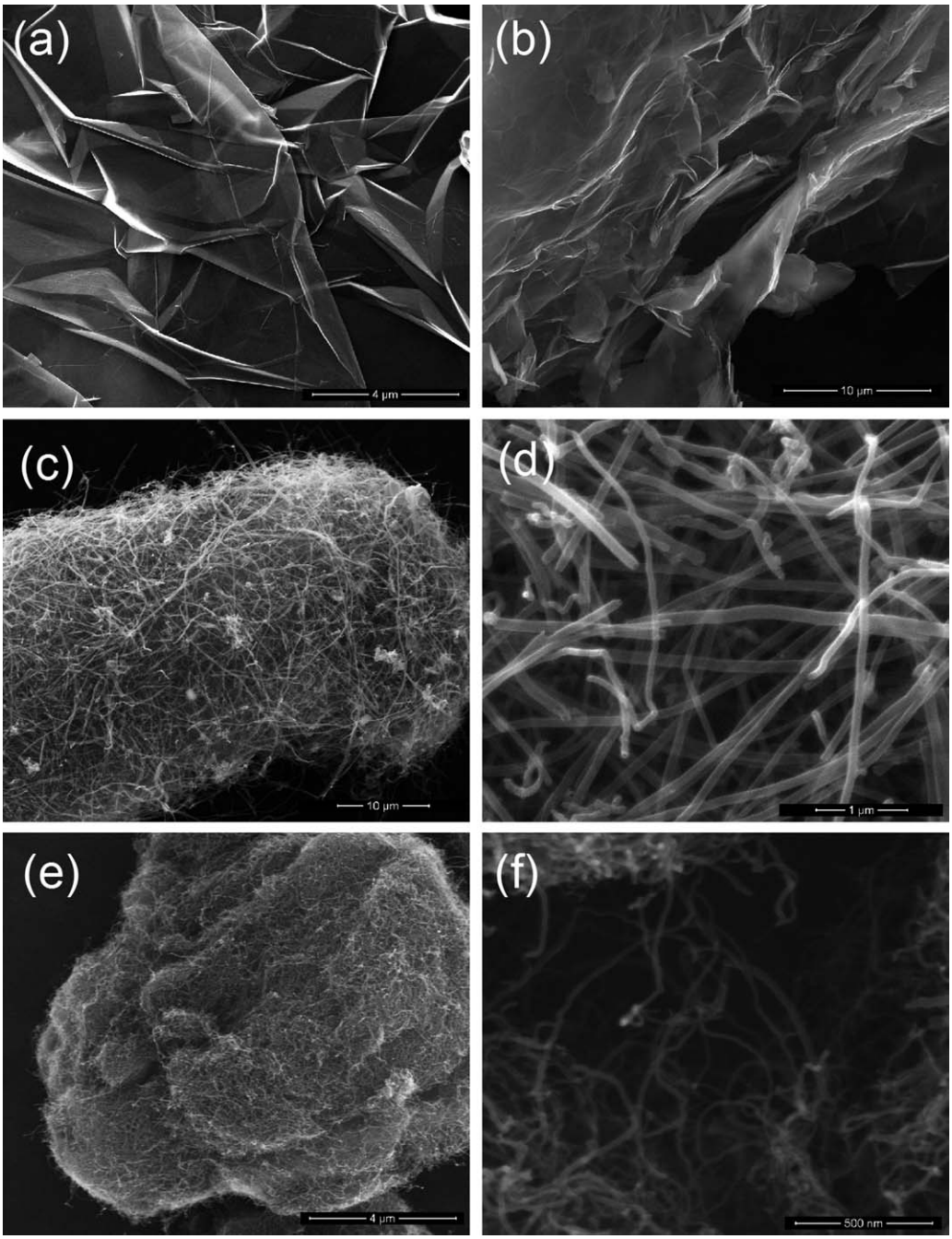

Figure 1. SEM images of (a,b) EG, (c,d) CNF, and (e,f) CNT.

together forms multiple contact points. It can be concluded that the especially 1D nano fillers contribute to the connection of embedded large graphene sheets outlying each other. Figure 3(c,d) represent the microstructure of EG20CNF5CNT5 sample. In these images, it is obviously seen that the dispersed EG platelets are thinner and exhibit relatively better adhesion with the polymer than the series of composites prepared with the EG only. Thinner EG platelets can be explained by the increasing of melt viscosity as a result of introducing of CNT and CNF into structure that yields relatively more intensive shear forces for peeling apart of EG sheets during processing. Better adhesion could be originated from the fact that the physical network formed by CNT and CNF into the polymer matrix possibly influenced the thermal expansion coefficient (k) which was related to the shrinking behavior of polymer by restricting the mobility of polymer chains. Consequently, it can be expected that the composites prepared with double and triple filler combinations show lower resistance than the single-filler counterparts due to the formation of multiple contact points and more conduction pathways for the electron transfer.

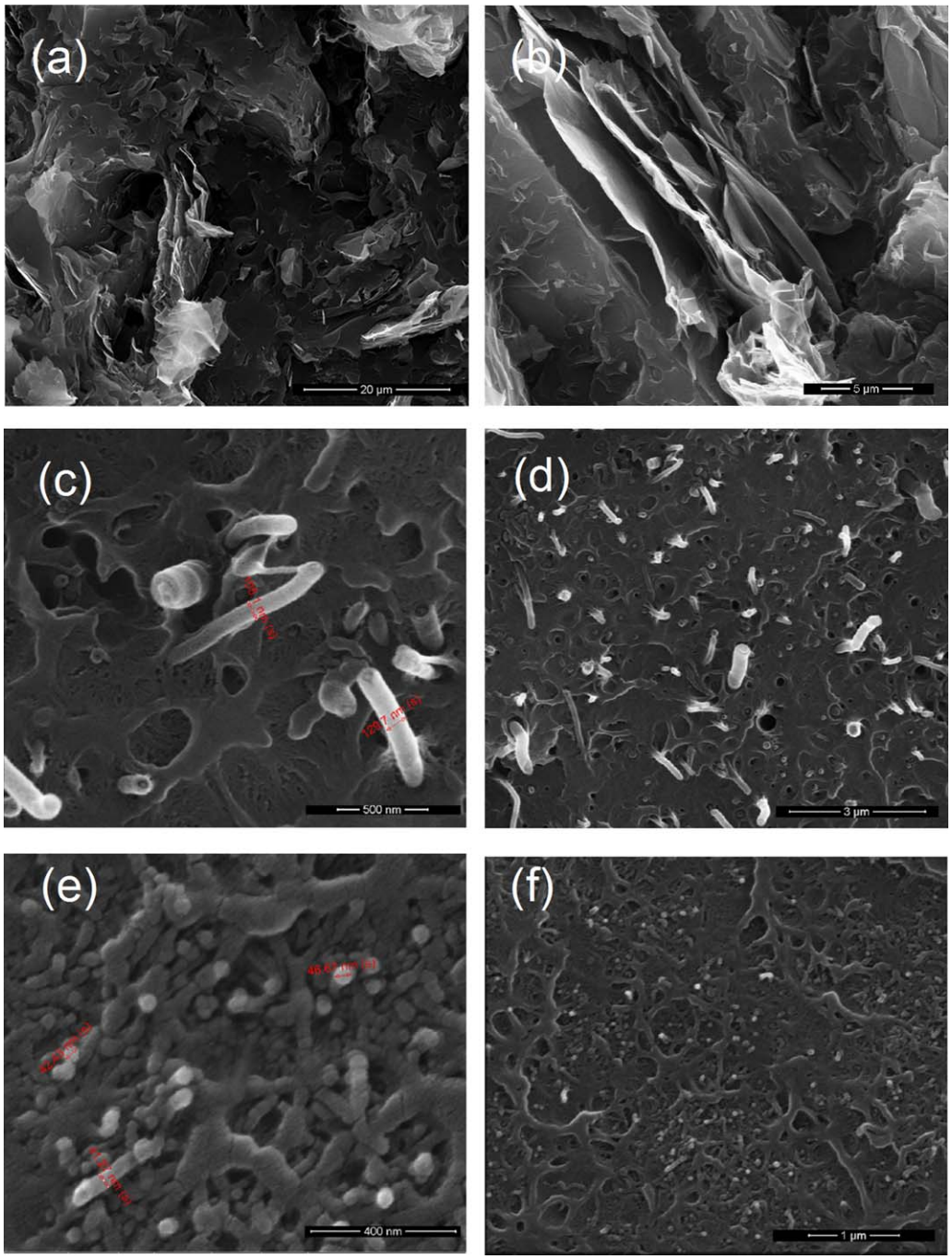

Figure 2. SEM images of (a,b) EG10, (c,d) CNF10, and (e,f) CNT5. [Color figure can be viewed in the online issue, which is available at wileyonlinelibrary.com.]

Mechanical Properties

DMA is the most widely used and practical method to investigate some mechanical and solid-state viscoelastic properties of polymers, blends, and composites in a wide range of temperature. The DMA measurements can also be used to determine the effect of compositional parameters on the viscoelastic properties of samples such as storage modulus (E'), loss modulus (E''), phase angle or damping factor (tan δ), and the transition temperatures such as glass transition (T_g) and melting (T_m). In general, solid-state viscoelastic properties of polymer composites are not only influenced by the structural properties of polymer matrix and the type and amount of fillers, but the polymer–filler and filler–filler interactions, geometry and dispersion quality of filler, and thermo-mechanical history of samples during processing also affect the viscoelastic properties of such materials. Therefore, the DMA data can be attentively used to reveal the micro-structural properties of composites.

Figure 4 shows the dependence of E' on the temperature for the sample series prepared with the EG, CNT, and CNF. It is evidently

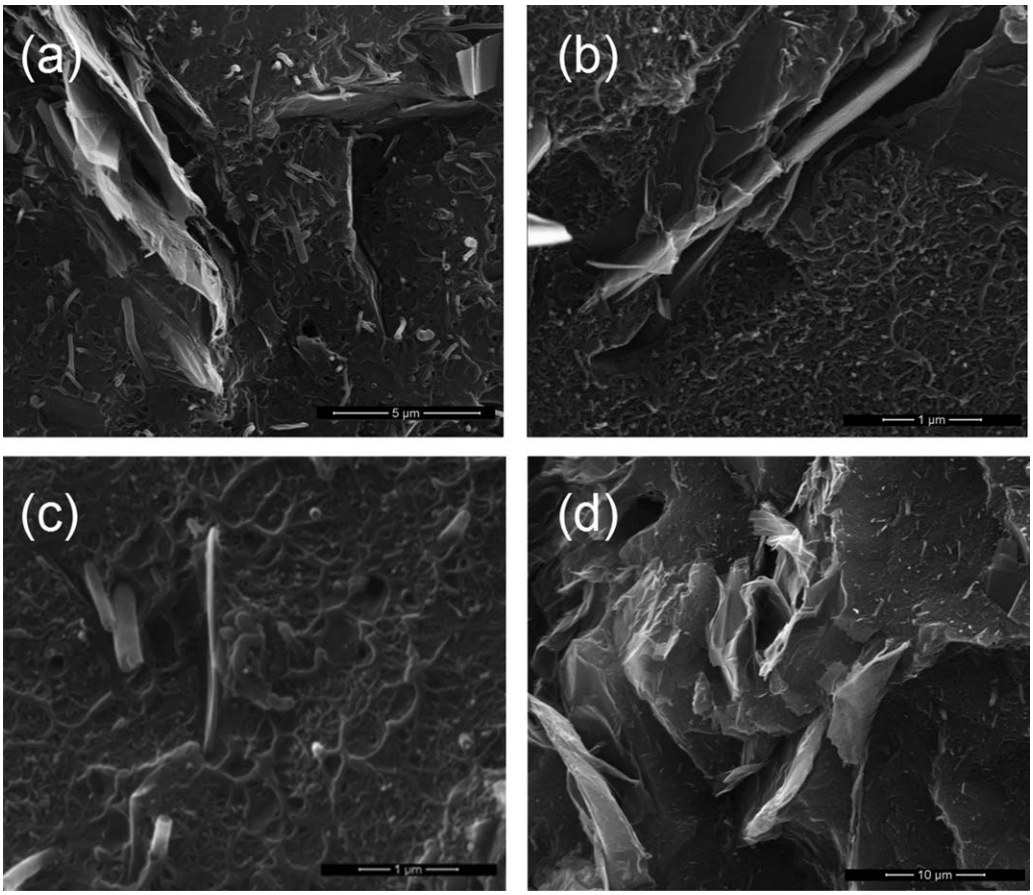

Figure 3. SEM images of (a) EG20CNF10, (b) EG20CNF10, and (c,d) EG20CNF5CNT5.

seen that the increasing amount of filler improve the E' values of all samples. But, this enhancement effect is more pronounced at the rubbery region. These results imply that the modulus in the glassy region is primarily determined by the polymer phases while the solid-state properties of composites mainly depend on the physical parameters of fillers in the rubbery region. This phenomenon has also been reported for other thermoplastic-based composite systems.[39–41] Thus, improvement in E' values in the rubbery region were used to quantify the effect of filler type and amount on the enhancement of mechanical properties of composites and the relative changes in the E' at 160°C were compared.

Figure 5 represents the dependence of relative modulus (E_R) on the ϕ_f for the series of samples prepared with the EG, CNT, and CNF. The E_R can be defined as the ratio of E' of composite to that of polymer. As seen in this figure, the E_R value significantly increased with the introducing of carbon nano fillers above the ϕ_f value of 0.02. It was found that the values of E_R decreased in the order of CNT>CNF>EG at a particular amount of carbon nano filler, especially at relatively higher amount of filler. The dramatic increase in the E_R values of series of samples was possibly originated from the higher filler–filler interaction at these compositions. It can also be concluded that the reinforcing effects of carbon nano fillers on the elastic modulus of composites decreased in the order of CNT>CNF>EG. Reinforcing effects of fillers on the physical properties of polymer composites including no compatibilizer can be quantified with the physical parameters of fillers such as geometry, loading amount, dispersion quality or aspect ratio, orientation issues etc. or the variations in the supramolecular features of polymer mainly degree of crystallinity. The aspect ratio of fillers is ordinarily accepted the most important parameter on the mechanical properties of composites. In general, higher A_f values indicate better filler dispersion for nanocomposites. The A_f value can be estimated indirectly by various approaches based on the rheological and mechanical behaviors and, in some cases, permeability performances of composites.[38,42,43] One of the most widely used approach to determine the A_f values of fillers in the polymer composites including non-spherical fillers is the modified-Guth model,[43] given in eq. (2).

$$E_c = E_p(1+0.67A_f.\phi_f+1.62A_f^2.\phi_f^2) \quad (2)$$

The modified-Guth model is a simple parabolic function expressed the relationship between the E_R and ϕ_f. Fitting curves for the series of samples prepared with various types of carbon nano fillers are shown in Figure 6. As seen in the Figure, the modified-Guth model can successfully fit the E_R values of composites at 160°C depending on the type and amount of filler. The calculated A_f values of the fillers were found to be 27, 50, and 75 for the EG, CNF, and CNT, respectively. It is definitely

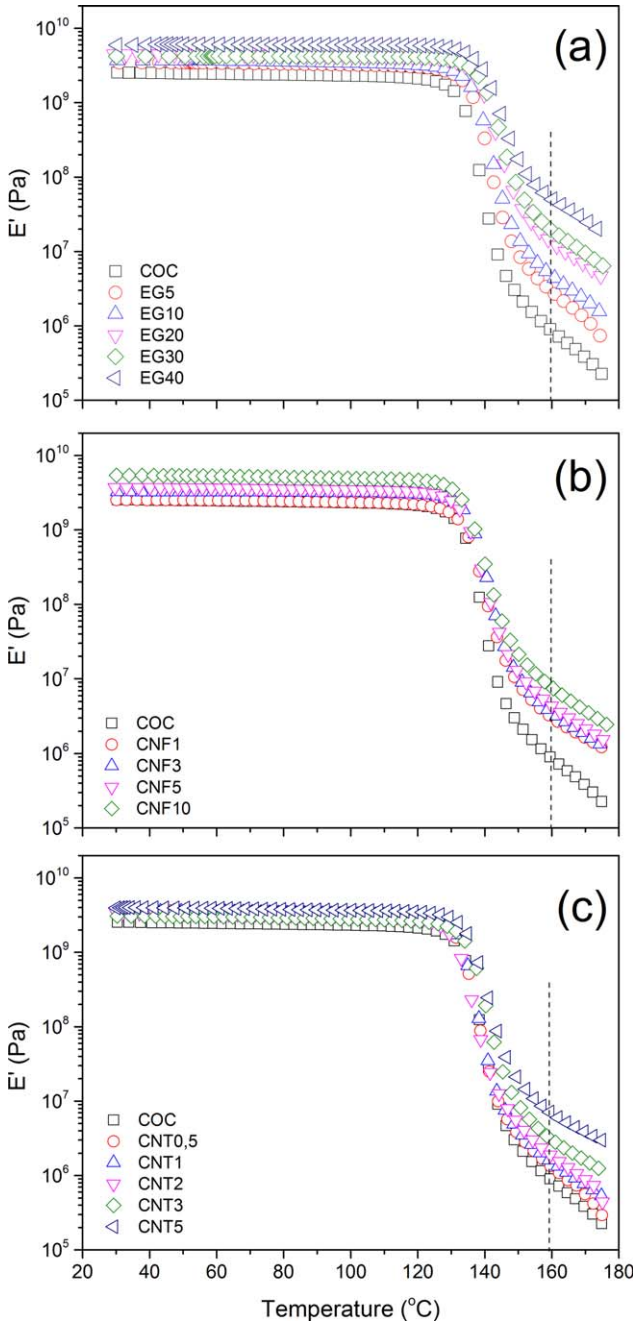

Figure 4. Dependence of storage modulus (E') on the temperature for the composite samples prepared with the various type and amount of fillers, (a) EG, (b) CNF, and (c) CNT. [Color figure can be viewed in the online issue, which is available at wileyonlinelibrary.com.]

seen that the calculated A_f values of samples prepared with the CNF and CNT are much lower than the values predicted with the SEM images and calculated with the producer data. It has been supposed that the lower A_f values are possibly due to the agglomeration of the fillers because of increasing of filler–filler interactions at relatively higher amount of loading and breaking of the tubular and fibrillar fillers during melt processing.

In this study, DMA data of samples prepared with the double and triple-filler combinations were also used to testify the evi-

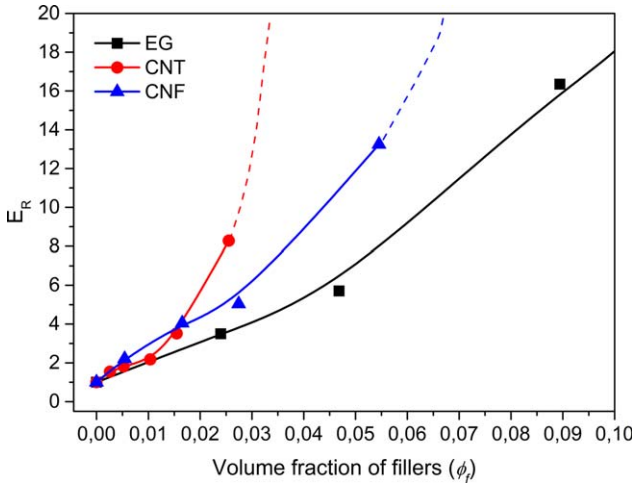

Figure 5. Dependence of relative modulus (E_R) on the volume fraction of filler (ϕ_f). [Color figure can be viewed in the online issue, which is available at wileyonlinelibrary.com.]

dences of better adhesion between graphitic nano sheets and polymer matrix mentioned before. This approach is based on the monitoring of longitudinal displacement (dL) of sample as a function of temperature and comparing of dL curves depending on the filler type and/or sample composition. It is known that the DMA measurements provide the absolute displacement in uniaxial tensile mode. This was also the technical reason for why the DMA measurements were performed in the tension geometry. It was due to the recording of absolute longitudinal displacements of samples precisely, depending on the temperature. The determination of thermal expansion coefficient (k) of solid materials is also based on the measuring of volume or length changes (expansion or contraction) of a specimen with the temperature in a thermo-mechanical analyzer (TMA). The k (K^{-1}) reported as the relative displacement value (dL/L) for unit in temperature in K, simply defined as following;

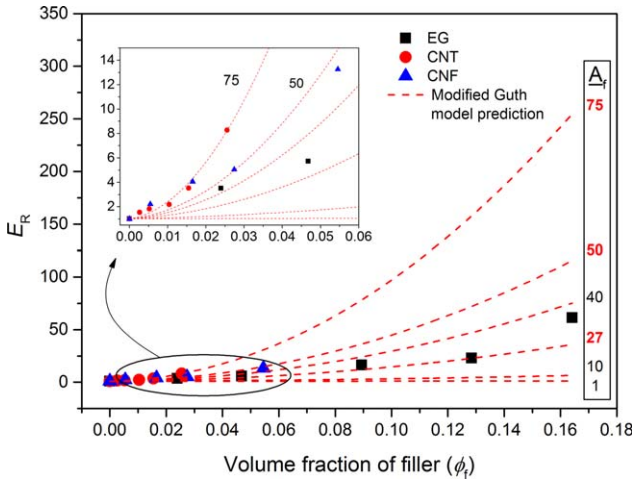

Figure 6. Estimation of aspect ratio (A_f) values of fillers by the modified-Guth model. [Color figure can be viewed in the online issue, which is available at wileyonlinelibrary.com.]

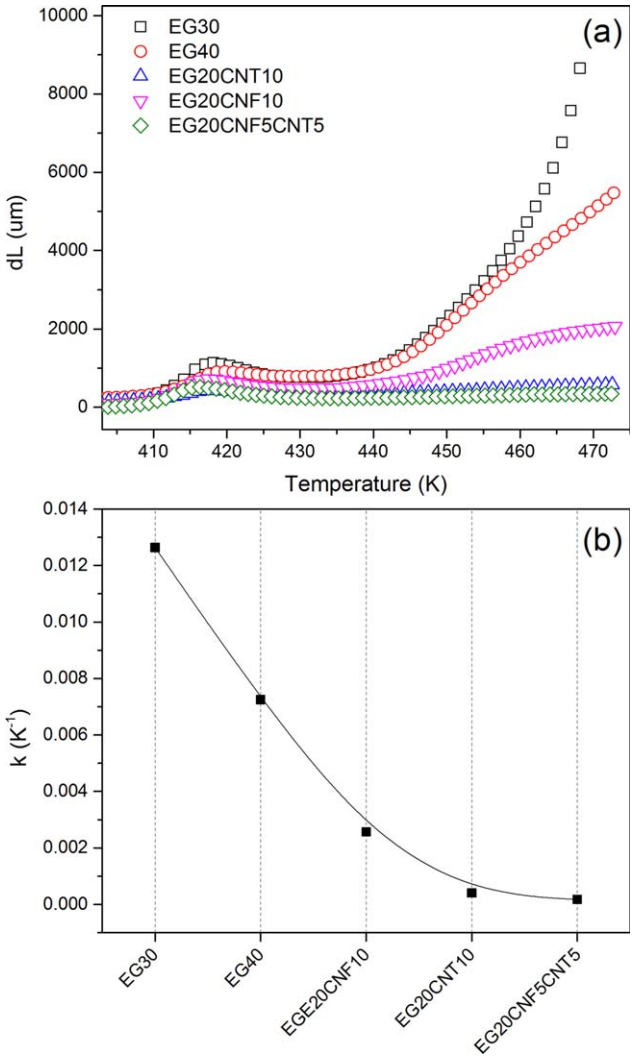

Figure 7. (a) Comparing of uniaxial displacement for the samples including the total filler amount of 30 phr, recorded at DMA test and (b) estimated thermal expansion coefficient (k) based on the displacement above the glass-transition temperature. [Color figure can be viewed in the online issue, which is available at wileyonlinelibrary.com.]

$$k(K^{-1}) = \frac{dL}{L}\frac{1}{K} \tag{3}$$

The k value can be calculated by plotting the displacement (dL) against temperature (T). Figure 7(a) shows the displacement of some samples as a function of temperature, in K. Small peaks around the temperature of 415 K point out the glass-transition of samples. As seen in the figure that the displacement varied in the glassy and rubbery regions, as expected. Especially, dL tremendously increased for the EG30 and EG40 above the T_g, indicated relatively high uniaxial expansion of these samples. This behavior is normally seen for all polymers, except highly cross-linked materials, due to the mobility of polymer chains. But, the higher expansion seen in the EG30 and EG40 could be stimulated by the self-lubricating effects of large graphitic nano sheets under the oscillating strain and poor interfacial adhesion between polymer and graphite platelets since these samples contain no compatibilizer. The k values calculated with the DMA

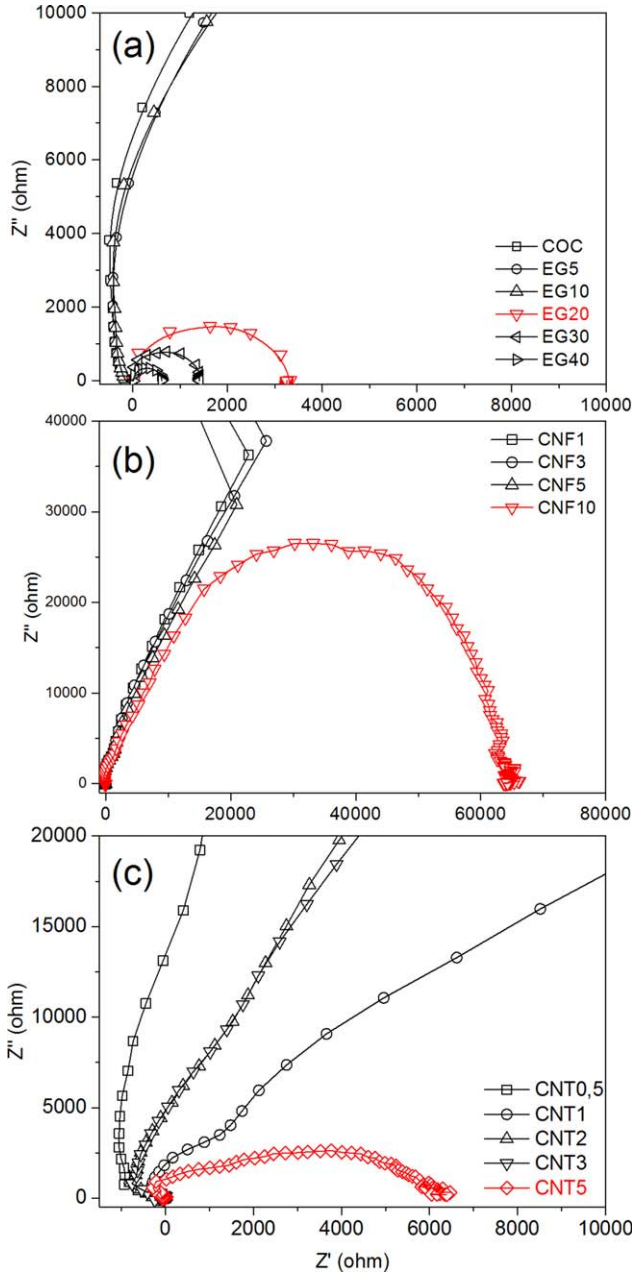

Figure 8. Nyquist plots of samples including various amounts of (a) EG, (b) CNT, and (c) CNT depending on the type and amount of fillers. [Color figure can be viewed in the online issue, which is available at wileyonlinelibrary.com.]

data according to the eq. (3) are given in Figure 7(b). When the uniaxial expansion behaviors and the k values of composites having the total filler amount of 30 phr are compared, it is seen that the introducing of high aspect ratio, 1D fillers into the sample composition dramatically reduces the expansion and resulting k values of composites. It was also found that the CNT was more effective than the CNF to decrease the thermal expansion by comparing the k values of EG20CNT10 and EG20CNF10. Consequently, the results given in this part have clearly proved the morphological evidences of composites prepared with the double and triple filler combinations and

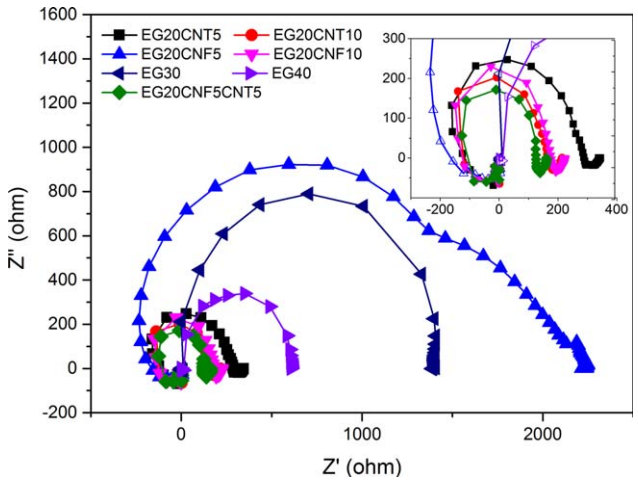

Figure 9. Comparing the Nyquist plots of samples including double and triple filler combinations with those of the EG30 and EG40. [Color figure can be viewed in the online issue, which is available at wileyonlinelibrary.com.]

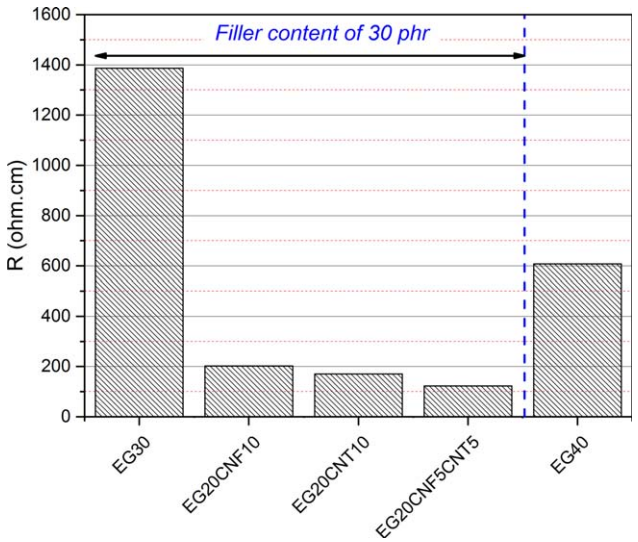

Figure 10. Comparing of bulk resistivity of samples including the total filler amount of 30 and 40 phr. [Color figure can be viewed in the online issue, which is available at wileyonlinelibrary.com.]

previously discussed in the "microstructural features of fillers and composites" section.

Electrical Properties of Samples

Electrical properties of the composites depending on the filler type, filler amount and the sample composition were determined by measuring the bulk resistance of samples with an impedance analyzer. The characteristic Nyquist plots, relationship between the real (Z') and imaginary (Z'') parts of complex impedance (Z^*), were measured as a function of frequency. It is accepted that the Z′ is related to capacitance while the Z″ refers to loss factor, in other word loss of accumulated charges or the conductive component. The real part of complex impedance at low frequency region or the diameter of semicircle can be accepted as the bulk resistance (R, ohm) of the test specimen. Figure 8 shows the Nyquist plots of series of samples prepared with the EG, CNF, and CNT. The Nyquist plots normally yield open or closed semicircles as seen in the given figures. Smaller diameter in the closed semicircles represents the lower the bulk resistance for samples. Figure 8 shows that some samples including relatively low amount of filler reveal open arcs in the whole frequency range employed. The open arcs imply that the bulk resistance of these samples is very high. Although it is possible to calculate the intrinsic bulk resistivity values of these samples by fitting of open arcs mathematically, the resistance values of samples shown a closed semi-circle have been further discussed in this study. The critical filler concentration in which the bulk resistance shows a significant decrease is called as the electrical percolation threshold. The electrical percolation threshold of CPCs can be determined with the formation of a closed semi-circle in the Nyquist plots. Based on this assumption, the electrical percolation thresholds for the series of samples prepared with the EG, CNF, and CNT were found to be 20, 10, and 5 phr, respectively. The various percolation thresholds for the series of samples can be attributed to the different geometrical features and thus the aspect ratio and dispersion quality of fillers. Figure 8(a) shows that the Nyquist diagrams of EG5 and EG10 are similar to that of COC which signifies that the bulk resistances of these composites are probably close to that of neat polymer (10^{14} ohm.cm). However, the composites prepared with the same or less amount of CNT or CNF (e.g. CNT5 and CNF10) exhibit much lower bulk resistance than the EG10. The higher bulk resistance of EG10, compared to those of CNT5 and CNT10, could be explained by the lack of conductive pathways throughout the graphite nano platelets in this sample.

Based on the bulk resistance values of samples, composite structure was then formulated by introducing of double and triple combinations of carbon nano fillers to decrease the resistivity at the same or lower amount of filler. The compositions of multi-filler samples were designed by considering of processing parameters, costs, and geometrical properties of fillers. All the fillers were employed about the individual percolation thresholds. It was also aimed that the conductive path was mainly formed by the 20 phr of EG in all multi-filler samples because the graphite is much cheaper than the CNT and CNF, commercially available and also acts as a processing aid in the melt-state in a twin screw extrusion due to its solid-lubricant property. Figure 9 represents the Nyquist plots of some multi-filler composites to those of EG30 and EG40. The calculated bulk resistance values of samples are also compared in Figure 10. As seen in the Figure 9 that the semicircle diameters and corresponding bulk resistance of EG20CNT10 (181 ohm.cm) and EG20CNF10 (192 ohm.cm) samples were found to be lower than those of EG30 (1400 ohm.cm) and EG40 (607 ohm.cm). This decrease in the bulk resistance could be attributed to the facts; (i) formation of multiple conduction pathways between the large graphite sheets via a 1D filler and (ii) reducing of interfacial gaps between the EG platelets and polymer matrix which includes 1D conductive filler to transfer electrons easily by hoping mechanism, as verified in Figure 3. The lowest bulk resistivity value of 125 ohm.cm was obtained for the sample

prepared with the triple filler combination, denoted as EG20CNF5CNT5. Although the introducing of CNT was more effective than that of CNF into the EG20 composites for decreasing of resistivity, it was found that the using of 5 phr CNF and CNT, instead of 10 phr of CNT, lead to reduce the bulk resistance. This result shows that the using of small amount of CNF and CNT in the EG (or graphite) filled CPCs shows a great impact and a synergistic effect to decrease the bulk resistance of composite. Employing of triple filler combination is also important because it allows using less amount of CNT which is one of the most expensive carbon nano fillers with the lack of commercial scale mass-production yet in addition to the technical advantage of this formulation on resistivity.

CONCLUSION

In this study, microstructural features, mechanical properties, and bulk resistances of thermoplastic composites prepared with the various amount of EG, CNT, and CNF were investigated. Relationships between the filler geometry, aspect ratio, and physical properties of composite were quantified. The lowest percolation threshold for electrical conductivity was obtained with the CNT as 5 phr. However, the theoretical A_f value of CNF was much higher than that of CNT according to the producer information, it was found that the actual A_f of CNT was higher than that of CNF based on the mechanical properties of samples. On the other hand, the 1D carbon nano fillers dramatically reduced the temperature-dependent uniaxial expansion of composites under tensile forces. It has been concluded that the replacing of some part of EG with the 1D nano fillers into the composite structure significantly decreased the bulk resistivity of samples. Consequently, it has been suggested that the double and/or triple combinations of conductive fillers could be employed into the compositions of polymer based conductive composites to design the physical performance of composites, processing difficulties and cost issues.

ACKNOWLEDGMENTS

This study was supported by TUBITAK, The Scientific and Technological Research Council of Turkey, with the grant number of 114M081.

REFERENCES

1. Cao, Z. Y.; Wei, B. Q. *ACS Nano* **2014**, *8*, 3049.
2. Varzi, A.; Taubert, C.; Wohlfahrt-Mehrens, M. *Electrochim Acta* **2012**, *78*, 17.
3. Caglar, B.; Fischer, P.; Kauranen, P.; Karttunen, M.; Eisner, P. *J. Power Sources* **2014**, *256*, 88.
4. Sun, Y.; Shi, G. *J. Polym. Sci. B Polym. Phys.* **2012**, *51*, 231.
5. Sonoda, K.; Moriya, Y.; Jantunen, H. *Mater. Sci. Poland* **2011**, *29*, 63.
6. Bishay, I. K.; Abd-El-Messieh, S. L.; Mansour, S. H. *Mater. Des.* **2011**, *32*, 62.
7. Stassi, S.; Canavese, G. *J. Polym. Sci. B Polym. Phys.* **2012**, *50*, 984.
8. Sarvi, A.; Sundararaj, U. *Synthetic Met.* **2014**, *194*, 109.
9. Vovchenko, L.; Lazarenko, O.; Matzui, L.; Perets, Y.; Zhuravkov, A.; Fedorets, V.; Le Normand, F. *Phys. Status Solidi A* **2014**, *211*, 336.
10. Pour, S. A. H.; Pourabbas, B.; Hosseini, M. S. *Mater. Chem. Phys.* **2014**, *143*, 830.
11. Farimani, H. E.; Ebrahimi, N. G. *J. Appl. Polym. Sci.* **2012**, *124*, 4598.
12. Pham, G. T.; Park, Y. B.; Liang, Z.; Zhang, C.; Wang, B. *Compos. B Eng.* **2008**, *39*, 209.
13. Zhao, Y. F.; Xiao, M.; Wang, S. J.; Ge, X. C.; Meng, Y. Z. *Compos. Sci. Technol.* **2007**, *67*, 2528.
14. Li, K.; Dai, K.; Xu, X. B.; Zheng, G. Q.; Liu, C. T.; Chen, J. B.; Shen, C. Y. *Colloid Polym. Sci.* **2013**, *291*, 2871.
15. Kasgoz, A.; Akin, D.; Durmus, A. *Compos. B Eng.* **2014**, *62*, 113.
16. Al-Saleh, M. H.; Gelves, G. A.; Sundararaj, U. *Mater. Design* **2013**, *52*, 128.
17. Micaela, C.; Alessandro, C.; Imran, S. M.; Vitthal, J. P.; Alberto, T. *Compos. Appl. Sci. Manuf.* **2014**, *61*, 108.
18. Yu, B.; Xu, X. C. *RSC Adv.* **2014**, *4*, 3966.
19. Sulong, A. B.; Ramli, M. I.; Hau, S. L.; Sahari, J.; Muhamad, N.; Suherman, H. *Compos. B Eng.* **2013**, *50*, 54.
20. Zhang, X. H.; Liang, G. Z.; Chang, J. F.; Gu, A. J.; Yuan, L.; Zhang, W. *Carbon* **2012**, *50*, 4995.
21. Safdari, M.; Al-Haik, M. *Nanotechnology 2012*, 23.
22. He, Z.; Zhang, B.; Zhang, H.-B.; Zhi, X.; Hu, Q.; Gui, C.-X.; Yu, Z.-Z. *Compos. Sci. Technol.* **2014**, *102*, 176.
23. Srivastava, S.; Tchoudakov, R.; Narkis, M. *Polym. Eng. Sci.* **2000**, *40*, 1522.
24. Lee, T.-W.; Jeong, Y. G. *Compos. Sci. Technol.* **2014**, *103*, 78.
25. Ma, C. G.; Xi, D. Y.; Liu, M. *J. Compos. Mater.* **2013**, *47*, 1153.
26. Zhao, S. G.; Zhao, H. J.; Li, G. J.; Dai, K.; Zheng, G. Q.; Liu, C. T.; Shen, C. Y. *Mater. Lett.* **2014**, *129*, 72.
27. King, J. A.; Barton, R. L.; Hauser, R. A.; Keith, J. M. *Polym. Compos.* **2008**, *29*, 421.
28. Ma, P.-C.; Liu, M.-Y.; Zhang, H.; Wang, S.-Q.; Wang, R.; Wang, K.; Wong, Y.-K.; Tang, B.-Z.; Hong, S.-H.; Paik, K.-W.; Kim, J.-K. *ACS Appl. Mater. Inter.* **2009**, *1*, 1090.
29. Thongruang, W.; Spontak, R. J.; Balik, C. M. *Polymer* **2002**, *43*, 2279.
30. Clingerman, M. L.; Weber, E. H.; King, J. A.; Schulz, K. H. *Polym. Compos.* **2002**, *23*, 911.
31. Du, F.; Fischer, J. E.; Winey, K. I. *Phys. Rev. B* **2005**, *72*, 121404.
32. Das, N.; Chaki, T.; Khastgir, D. *Carbon* **2002**, *40*, 807.
33. Mamunya, E.; Davidenko, V.; Lebedev, E. *Compos. Interf.* **1996**, *4*, 169.
34. Karasek, L.; Sumita, M. *J. Mater. Sci.* **1996**, *31*, 281.
35. Ban, H. T.; Shigeta, M.; Nagamune, T.; Uejima, M. *J. Polym. Sci. Part A: Polym. Chem.* **2013**, *51*, 4584.
36. Akin, D.; Kasgoz, A.; Durmus, A. *Compos. A* **2014**, *60*, 44.
37. Motlagh, G. H.; Hrymak, A. N.; Thompson, M. R. *J. Polym. Sci. Part B: Polym. Phys.* **2007**, *45*, 1808.

38. Kasgoz, A.; Akın, D.; Ayten, A. I.; Durmus, A. *Compos. B* **2014**, *66*, 126.
39. Pothan, L. A.; Oommen, Z.; Thomas, S. *Compos. Sci. Technol.* **2003**, *63*, 283.
40. Manikandan Nair, K.; Thomas, S.; Groeninckx, G. *Compos. Sci. Technol.* **2001**, *61*, 2519.
41. Sung, Y.; Kum, C.; Lee, H.; Byon, N.; Yoon, H.; Kim, W. *Polymer* **2005**, *46*, 5656.
42. Durmus, A.; Kasgoz, A.; Macosko, C. W. *Polymer* **2007**, *48*, 4492.
43. Kalaprasad, G.; Joseph, K.; Thomas, S.; Pavithran, C. *J. Mater. Sci.* **1997**, *32*, 4261.